[5]D. L. Martin, Phys. Rev. 176, 790 (1968).
[6]D. L. Martin, Phys. Rev. 141, 576 (1966); 170, 650 (1968).
[7]M. Hansen and K. Anderko, *Constitution of Binary Alloys*, (McGraw-Hill, New York, 1958).
[8]R. P. Elliot, *Constitution of Binary Alloys* (McGraw-Hill, New York, 1965), Suppl. 1.
[9]H. Iwasaki, J. Phys. Soc. Japan 17, 1620 (1962).

PHYSICAL REVIEW B VOLUME 4, NUMBER 12 15 DECEMBER 1971

Photoemission from Core States of Cs and Rb†

R. G. Oswald and T. A. Callcott
Department of Physics, The University of Tennessee, Knoxville, Tennessee 37916
(Received 6 July 1971)

Photoemission yields and electron energy distributions of Rb and Cs for photon energies of 12–22 eV are reported. Over most of this energy range, photoexcitation from $np^5(^2P_{3/2})$ $(n+1)s$ and $np^5(^2P_{1/2})$ $(n+1)s$ core levels is observed to be at least two orders of magnitude larger than excitation from the conduction band [$n=4$ (Rb), $n=5$ (Cs)]. Two peaks in the energy distributions which move to higher energy with increasing photon energy result from electrons being directly excited from the shallow core levels. A third peak, which remains stationary in energy position for all photon energies, results from Auger processes which refill the core levels. From the positions and shapes of the peaks, we have obtained values of the spin-orbit splitting of the core levels, the position of the core levels relative to the Fermi (or vacuum) level, and an estimate of the widths of the conduction band. Measurements of spectral yield show a threshold at the core-level–to–Fermi-level spacing that is consistent with this interpretation of structure in the energy distributions. Additional structure in the distributions results when an electron initially excited into one of the above peaks loses energy in exciting a surface plasmon as it escapes through the surface.

I. INTRODUCTION AND CONCLUSIONS

At photon energies below 25 eV, the photoemission process in metals usually involves photoexcitation from the filled portion of the conduction band followed by transport to and escape through the surface. The photoemission studies of Cs and Rb reported by Smith and co-workers, which extended to photon energies of 11.2 eV, followed this pattern.[1,2] At these energies, photoexcitation from rather narrow conduction bands (~1.5 eV for Cs, ~2.0 eV for Rb) injects electrons into higher-band states with this spread of energies. Some of these electrons escape without energy loss to form the highest-energy peak in the external distribution with approximately the width of the filled conduction band. Others escape after electron-electron collisions or after the generation of plasmons degrades their energy. Of particular interest is the fact that some electrons escape after exciting a single surface plasmon, and produce a peak (or shoulder) in the energy distributions displaced below the unscattered peak by the energy of the surface plasmon.

Another feature of interest at energies below 12 eV is that photoemission yields are very low and decrease steadily at photon energies well above the plasma frequency of the alkalies (3 eV in Cs and 3.4 eV in Rb). The low yield results from the fact that at energies above the plasma frequency, the alkalies become nearly transparent so that relatively few electrons are excited sufficiently close to the surface to escape into vacuum. It is well established, both experimentally and theoretically, that the alkalies are nearly free-electron metals with weak and decreasing optical absorption above their plasma frequencies.[3-5] Other absorption mechanisms involving joint excitation of plasmons and electrons have been proposed on the basis of optical measurements, but their existence would not alter the above conclusion that relatively few electrons are excited within the escape depth for photoemission.[5]

The photoemission measurements reported here for photon energies from 12 to 22 eV show many new features not observed at lower energies. Above a threshold of 12.2 eV in Cs and 14.1 eV in Rb, there is a sharply rising increase in yield throughout the entire energy range. Using a detailed analysis of the energy distributions of the electrons contributing to this increased yield, we draw the following conclusions about the processes contributing to photoemission in this energy range:

(a) Two peaks which are visible in our photoemission energy distributions (PED's) result from direct excitation of electrons from two shallow core levels located 12.3 and 14.2 eV below the Fermi level in Cs and 15.3 and 16.4 eV below the Fermi level in Rb. These levels are identified with the $np^5(^2P_{3/2})$ $(n+1)s$ and $np^5(^2P_{1/2})$ $(n+1)s$ excited states observed in the spectra of singly ionized Cs and Rb.[6] The spin-orbit splitting between levels of 1.9 eV for Cs

and 1.1 eV for Rb agrees with the value observed in the singly ionized Cs and Rb spectra. In the case of Cs, where the peaks are well separated in energy as compared to the peak width, the relative magnitudes of the peaks are found to be approximately 1:2, in agreement with the relative degeneracy of the two levels.

(b) Additional electrons for photoemission are produced when the higher of the two core levels is refilled by an Auger process, in which one conduction-band electron refills the core level and a second is excited by an equal energy and escapes into vacuum [see Fig. 6(b)]. Using a simple model we have obtained an estimate of the width of the filled conduction band from the observed width of this Auger peak. The values of 1.5 ± 0.2 eV obtained for Cs and 2.1 ± 0.2 eV for Rb are in good agreement with theoretical values.[7] The results summarized above are collected in Table I along with values of the same quantities derived from other studies.

(c) No electrons are observed in the PED's that result from a similar Auger recombination to the lower core level. We believe these to be refilled by a Coster-Kronig process that proceeds with at least an order of magnitude larger probability than the normal Auger process [see Fig. 6(b)].

(d) Both direct transitions and the Auger process inject electrons into higher-energy states with a relatively narrow spread of energies, just as does direct excitation from the conduction band at lower photon energies. Subsequent modification of the electron energies by scattering and plasmon generation is essentially the same as that observed by Smith and Spicer and described briefly above.

Section II of this paper describes the experimental equipment and procedures used in this study and Sec. III presents the data and analysis that leads us to the above conclusions.

II. EXPERIMENTAL TECHNIQUES

The photoemission apparatus consisted of the ion- and sublimation-pumped ultrahigh-vacuum chamber (shown schematically in Fig. 1), a vacuum monochromator, and electronic detection equipment.

At photon energies above 11 eV, light was admitted to the chamber through a 1000-Å-thick window of Sn or In. Sn of this thickness transmits more than 25% of incident light between 450 and 870 Å, while In is more than 20% transmitting between 770 and 1050 Å. Gesell has described the optical properties and preparation techniques for the films.[7] Because the windows are extremely fragile, the experimental chamber must be reduced to its working pressure in the 10^{-10}-Torr range with the window withdrawn and a straight-through metal-sealed valve sealing the port. After the monochromator is in place and evacuated, the window is inserted and sealed and the straight-through valve opened. A window holder built into a double-sided $2\frac{3}{4}$-in. flange was designed for this purpose.

Light was provided by a McPherson 235 scanning monochromator fitted with a windowless gas-discharge lamp. A spark discharge in N_2 provided five intense lines in the energy range from 11 to 16 eV. A 600-line/mm grating and 0.5-mm slits gave an energy spread of about 0.2 eV in the light incident on the sample. A dc discharge in Ne and He produced lines at 16.8 and 21.2 eV, respectively. When using these gases, the monochromator grating was replaced by a gold mirror to obtain a tenfold increase in intensity. When operated in this fashion, the energy spread at the sample is just the natural width of the Ne and He lines and the thin

TABLE I. Results of the analysis of PED's for Cs and Rb.

		E_a (eV) $np^5(^2P_{3/2})(n+1)s$	E_b (eV) $np^5(^2P_{1/2})(n+1)s$	$E_b - E_a$ (eV)	E_F (eV) (Fermi energy)
Authors[a]	Cs	12.3 ± 0.2	14.2 ± 0.2	1.9 ± 0.1	1.5 ± 0.2
	Rb	15.3 ± 0.3	16.4 ± 0.3	1.1 ± 0.3	2.1 ± 0.2
Bearden and Burns[a,b] (β-ray spectrometer data)	Cs	11.4 ± 0.5	13.1 ± 0.5	1.7	
	Rb	14.0 ± 0.3	14.8 ± 0.4	0.8	
Moore[c] (optical-absorption data for singly ionized atom)	Cs	13.3	15.2	1.9	
	Rb	16.6	17.7	1.1	
Kenney[d] (calculation)	Cs				1.5
	Rb				1.9

[a]Core levels measured with respect to Fermi level.

[b]J. A. Bearden and A. F. Burr, Rev. Mod. Phys. 39, 125 (1967).

[c]C. E. Moore, Nat. Bur. Std. (U.S.) Circular No. 467 (unpublished). Energy levels measured with respect to ground state of singly ionized ion.

[d]J. F. Kenney, MIT Solid-State and Molecular Theory Group Quarterly Progress Report No. 66, 1967 (unpublished).

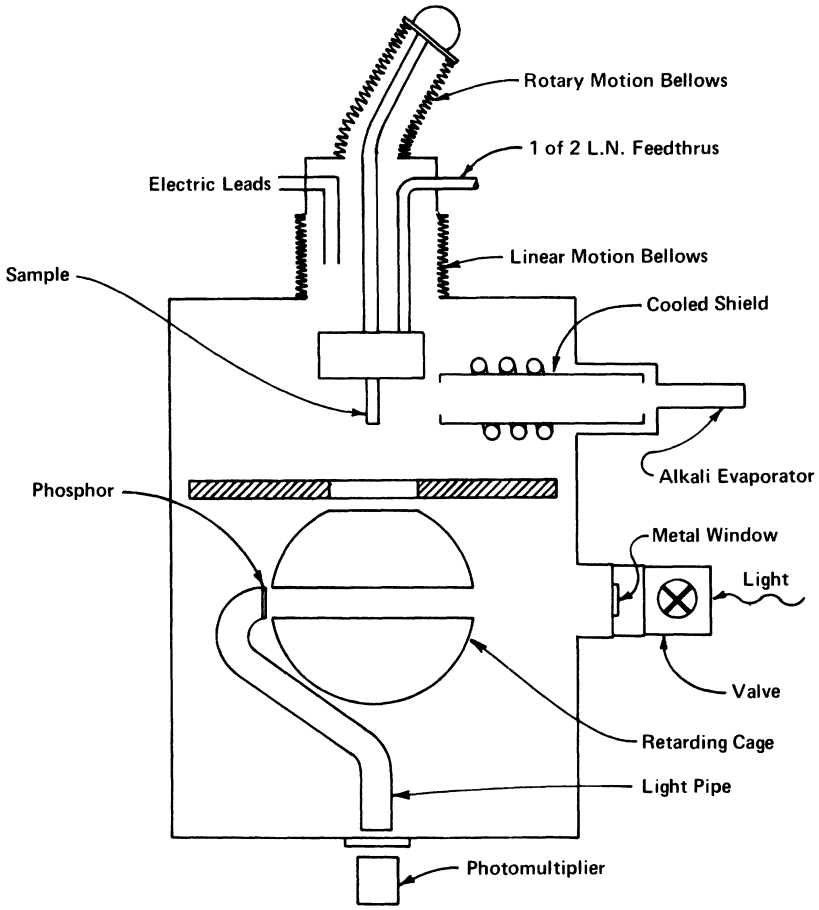

FIG. 1. Schematic diagram of sample chamber.

foil windows act as a bandpass filter to block other lines in the rare-gas spectra. Light intensity was measured with a sodium salicylate–coated light pipe that could be rotated in front of both the incident and reflected beams.

When the vacuum in the chamber reached the low 10^{-10}-Torr range (typically 2×10^{-10} Torr), as measured by a nude-ion gauge, a glass ampoule containing Cs or Rb was broken, and the metal was evaporated onto a liquid-nitrogen-cooled Pyrex substrate. During evaporation, the chamber pressure increased into the 10^{-7}-Torr range; it returned to about 2×10^{-9} Torr after evaporation. We believe that the residual gases after evaporation consisted mostly of alkali vapor and perhaps of Ne, He, or N_2 that leaked through microscopic pinholes in the metal-film window. During and after evaporation, the collimating baffles of the alkali gun were cooled to about 0°C to reduce the system pressure below the 10^{-6}-Torr vapor pressure of Cs (10^{-7} Torr of Rb) at room temperature. System contamination was reduced by intercepting all alkali vapor, not incident on the sample, by cooled baffles, and by separating the evaporation and measurement portions of the chamber with a metal plate.

For most films, no changes in the yield or energy distributions were observed for a period of several hours following evaporation. Completely specular films were never obtained. The frosty surface was composed of crystallites that slowly grew in size, especially when the film was warmed near the sublimation temperature. In time, larger crystallites would form.

Energy distributions were measured by placing a retarding potential between the sample and a 3-in.-diam. gold-plated spherical screen. The distributions were measured using the ac method described by Eden.[8] A typical PED was recorded in 4–5 min with a 0.5-V peak-to-peak ac signal superimposed on the retarding voltage.

With the above operating conditions, PED's taken at low energies had an excess width of about 0.7 eV, which may be attributed to the 0.5-V ac signal plus 0.2 eV of broadening due to energy spread in light from the monochromator, to variations in the collector work function, and to nonideal collector geometry. The width could be slightly reduced (~0.1 eV) by using narrower slit settings on the

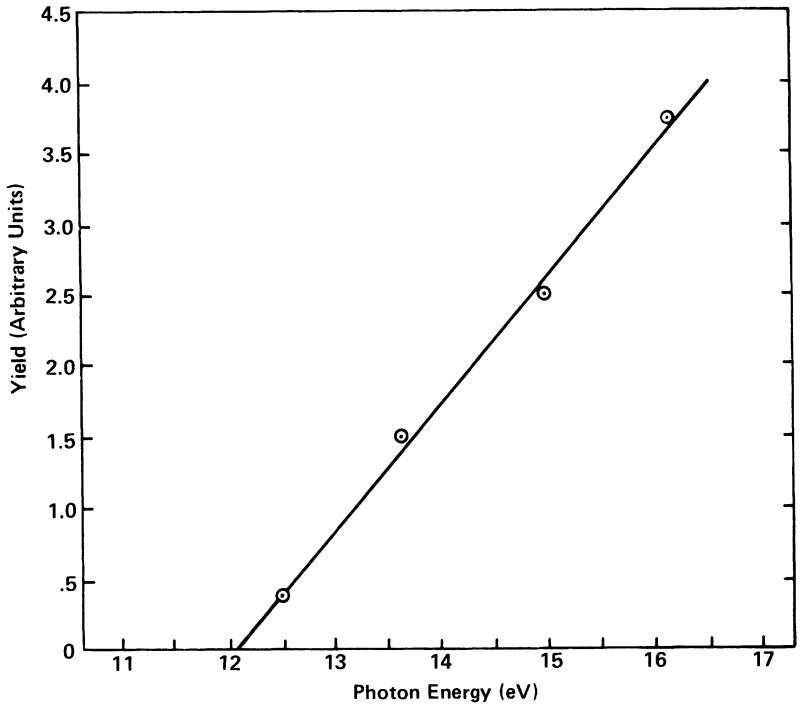

FIG. 2. Relative photoelectric yield for Cs plotted vs photon energy.

monochromator.

III. DATA AND ANALYSIS

As mentioned in Sec. I, we observed a sharp increase in yield at the threshold energy for core-level ionization. In Fig. 2 we plot the yield in arbitrary units for Cs as a function of photon energy. The intercept on the energy axis gives a threshold value of 12.2 eV. A value for the energy position of the upper-core level may be obtained from this threshold, which is in good agreement with the value obtained from measurements of photoemission peak positions discussed below.

Figures 3 and 4 are energy distributions for Rb and Cs. In these figures the zero of the kinetic-energy scale is set at the vacuum level. The curves are drawn to give equal magnitude to peak No. 1 and are not normalized to yield. Peak Nos. 2 and 3 result from the direct excitation of electrons from the two shallow core levels. These peaks shift position as the photon energy changes. This can be most clearly seen for peak No. 2 in the Cs distributions. Peak Nos. 1 and 4 and the upper edge all remain stationary as photon energy changes. The observation that the high-energy edge of the distributions does not change position with changing photon energy was quite unexpected and is rather an unusual effect in photoemission. Peak No. 1 is due to primary Auger electrons and peak No. 4 is associated with those Auger electrons which have generated plasmons.

The way we set the energy scale is worth comment. As noted above, there was a 0.7-eV excess width of the distributions recorded for photon energies below 10 eV. To compensate for the excess width in the distributions, we steepened both edges by removing 0.3 eV from the upper and lower edges. The lower intercept of the distribution was taken as a trial zero for the kinetic energy of the electrons. Using this energy scale and the analysis presented below, two independent values for the energy position of the core levels may be obtained. Small adjustments of the energy-scale zero (in no case exceeding 0.2 eV) were then made so that these two values were the same. The fact that the high-energy edge of the distributions was not determined by electrons photoexcited from the Fermi level, but by electrons produced in an Auger process, prevented us from using this edge and known photon energies and work functions to set the energy scale.

The shape of the Cs distributions can be accounted for by superimposing the three groups of electrons labeled A, B, and C in Fig. 5. Each group has a high-energy peak representing electrons that have escaped without energy loss and structure at lower energy representing electrons degraded by scattering or plasmon production. Each group, individually, closely resembles energy distributions observed at lower photon energies where the primary peak is produced by photoexcitation from the conduction band. Note that the primary peak height of A and B are approximately in the ratio of 1:2. We argue below that these peaks result from photoexcitation from core levels, with degeneracies in

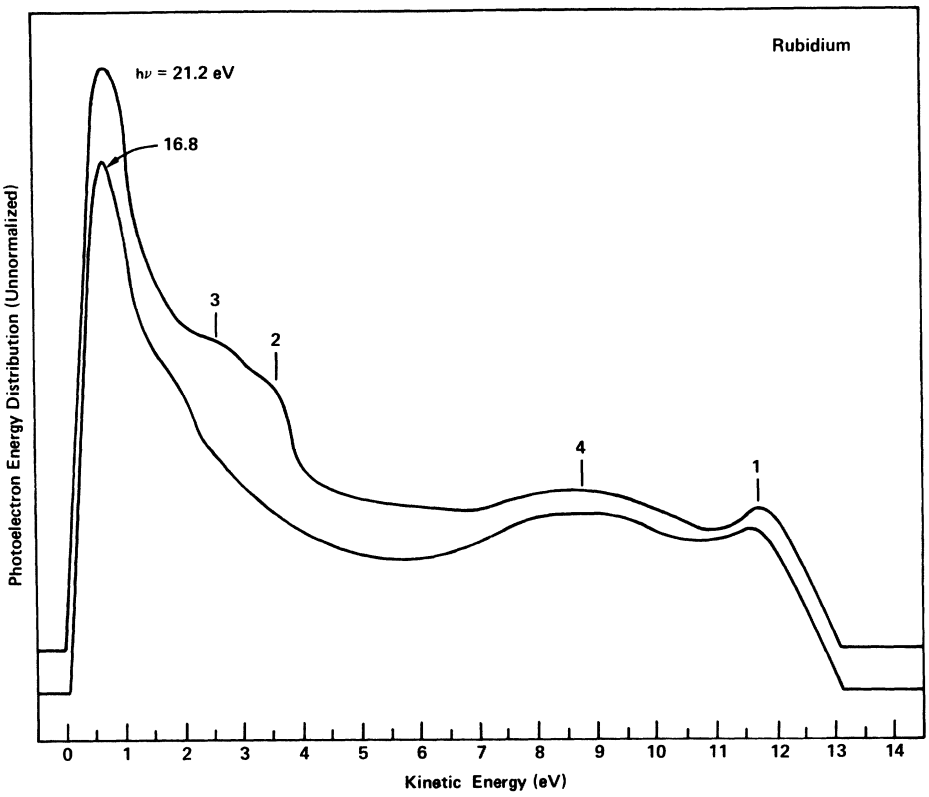

Fig. 3. Photoelectron energy-distribution curves for Rb plotted vs kinetic energy in vacuum.

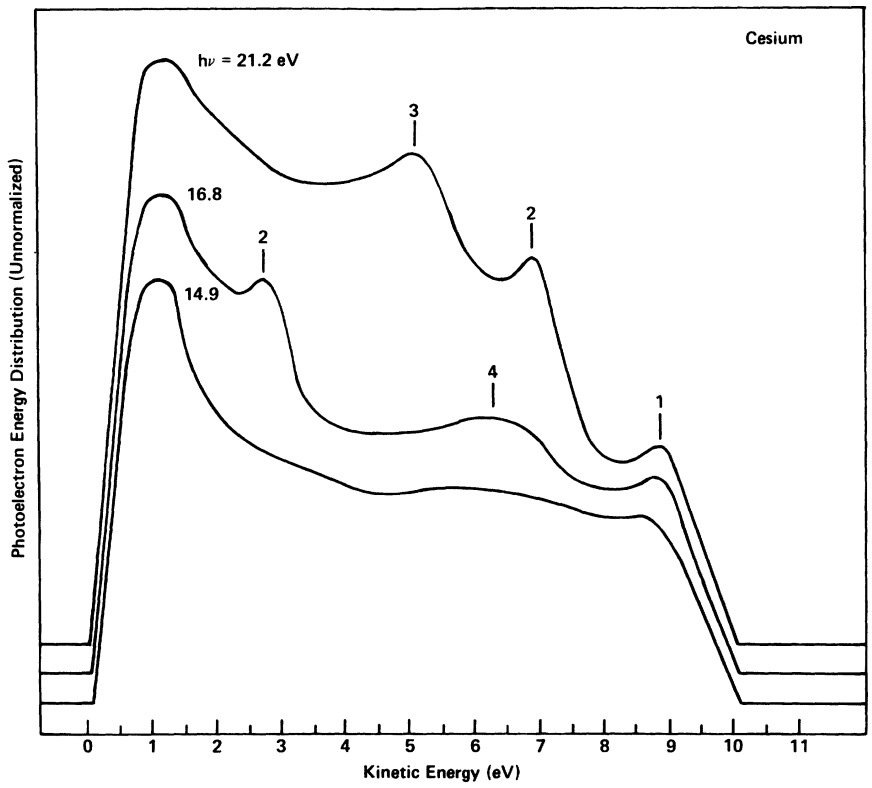

FIG. 4. Photoelectron energy-distribution curves for Cs plotted vs kinetic energy in vacuum.

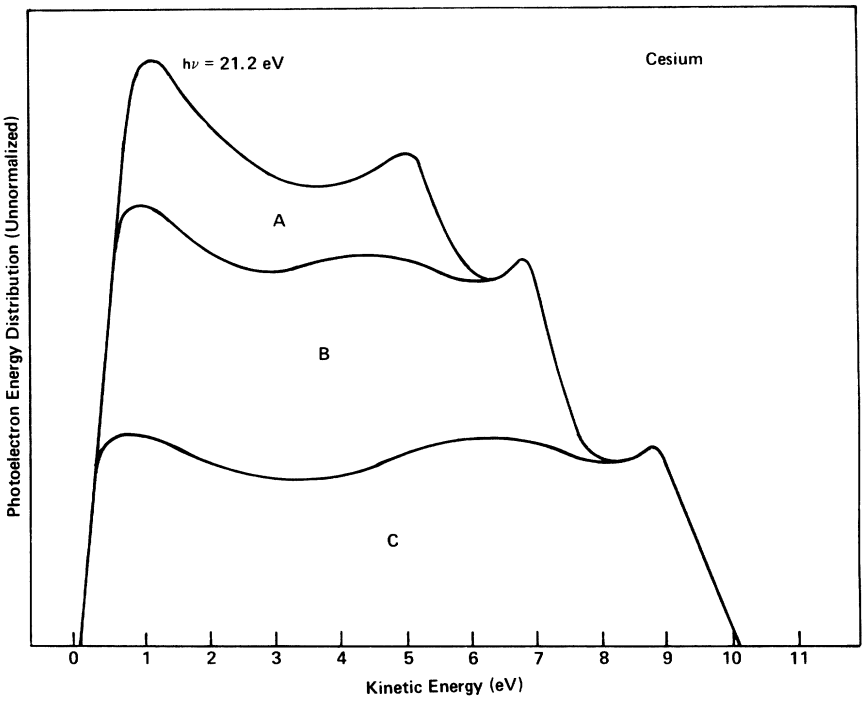

FIG. 5. Photoelectron energy-distribution curve for Cs plotted vs kinetic energy in vacuum. The shape of the distribution can be accounted for by superimposing the contributions of the scattered and primary electrons from photoexcitation (A and B) and Auger processes (C).

the ratio of 1:2.

The position of photoelectron peak No. 2 in the energy distributions is given by the equation

$$E_a' = \hbar\omega - E_a, \tag{1}$$

where E_a' is the kinetic energy of the photoelectrons in the peak with respect to the vacuum level, E_a is the position of the core level with respect to the vacuum level, and $\hbar\omega$ the photon energy. Figure 6(a) shows the photoelectron transitions. Another equation similar to (1) locates the position of photoelectron peak No. 3 in the distributions. From the splitting between the two peaks we determined the spin-orbit splitting of the core levels.

The electrons in peak No. 1 of the distributions are believed to result from the Auger process tagged (2) in Fig. 6(b). In this process, one electron from the conduction band fills a vacancy in the upper-core level, while a second electron is excited by an equal energy. The electrons at the upper edge of this Auger peak have an energy given by

$$E_{\text{edge}} = E_a - 2e\Phi, \tag{2}$$

where Φ is the work function of the material in volts and e the electronic change. $e\Phi$ was taken to be 1.8 eV for Cs and 2.0 eV for Rb.[9] The small changes of energy scale discussed above were made in order to obtain consistent values of E_a from Eqs. (1) and (2). Electrons from this Auger process are emitted into the vaccum as soon as vacancies are produced in the upper core level; thus, the threshold for photoemission, shown for Cs in Fig. 2, occurs at the energy separating the upper-core level and the Fermi level.

No electrons are observed that can be attributed to an Auger process of the above type going to the lower of the two core levels. We believe that this lower level is filled by the competing process tagged (1) in Fig. 6(b). This is a special type of Auger process, usually called a Coster-Kronig process in the literature.[10] This interpretation is supported by the fact that the Coster-Kronig process, when energetically permitted, commonly occurs with 1–3 orders of magnitude greater probability than competing Auger processes.[11] Energetic electrons produced by this process cannot escape in Rb and would appear at the extreme lower edge of the distribution in Cs.

Using a simple model of the Auger process and the Auger peak we are able to obtain an estimate of the width of the filled conduction band of Rb and Cs. A theoretical peak shape is calculated as follows. The energy of the excited Auger electron depends on the initial-energy states of both the excited electron and the electron which fills the hole in the upper-core state. If the matrix elements connecting the initial and final states of both electrons are assumed to be constant, then the number of electrons at energy E in the Auger peak is given by

$$N(E) \propto M_c M_f g(E_a) g(E) \int_0^E g(E') g(E'') dE', \tag{3}$$

where M_c is the transition matrix element between conduction-band electron states and core states,

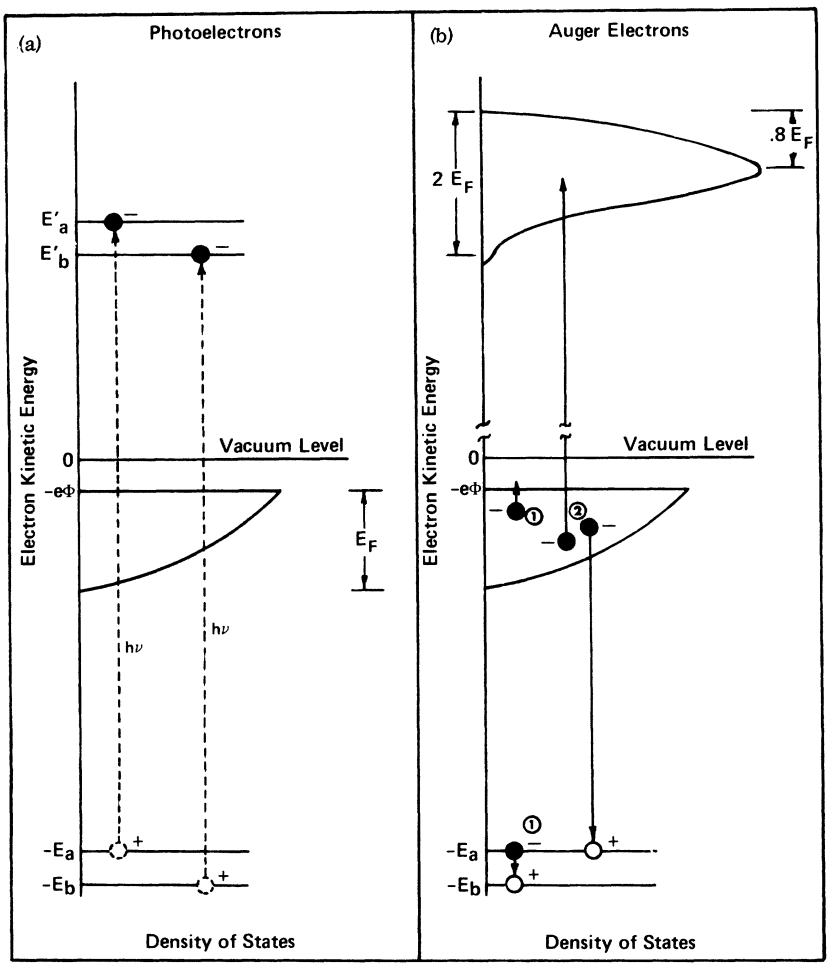

FIG. 6. Energy-level diagram for photo and Auger electrons. In (b) tag (1) is for the Coster-Kronig transitions and tag (2) is for the usual Auger transitions. At the top of (b) is a sketch of the calculated Auger electron peak.

M_f is the transition matrix element between conduction-band electron states and the final state of the excited electron, $g(E')$ is the initial-state density function for the electrons filling the hold in the core states, $g(E'')$ is the initial-state density function for the electrons making the Auger transition, $g(E)$ is the final-state density function for the excited electron and is assumed to be constant, and $g(E_a)$ is the state-density function for the core level and is assumed to have a value only at E_a.

For a free-electron Fermi gas with zero set at the bottom of the conduction band, the density functions have the following forms:

$$g(E') \propto \begin{cases} 0, & E' < 0\,, \quad E' > E_F \\ (E')^{1/2}, & 0 \leq E' \leq E_F \end{cases}$$

and

$$g(E'') = g(E - E' - E_a) \propto \begin{cases} 0, & E - E' - E_a < 0, \quad E - E' - E_a > E_F \\ (E - E' - E_a)^{1/2}, & 0 \leq E - E' - E_a \leq E_F. \end{cases}$$

When the density functions are substituted into Eq. (3), it is possible to evaluate the integral by standard techniques. Since E' and E'' both vary from 0 to E_F, it is necessary to perform the integration in two steps with limits going from 0 to $E - E_a$ and $E - E_a - E_F$ to E_F. We found the width of the Auger peak to be $2E_F$, with a maximum at $0.8E_F$ from the upper edge. The width of the conduction band (E_F) is then determined from the measurement of the separation of the peak and upper edge.

The values we have obtained for positions of core levels, their splittings and for conduction-band widths are given in Table I along with values obtained by other workers. Values obtained in the analysis of different experimental runs fall within 0.1 eV of the central values indicated, and thus well within the quoted error limits. The quoted experimental errors result from broadening of structural features by the resolution of the energy analyzer, and in the case of E_a and E_b from the precision with which we can set the energy scale. We have assumed that positions of structural features can normally be determined to within a fifth of the uncertainty in the width of the distribution.

In our analysis of the data we have assumed that the core-level energy positions are the same in the photoexcitation and Auger recombination processes. This implies that the final state of the Auger process is the same as the initial state of the excitation, i.e., that it results in a lattice ion in its "ground-state" configuration. This could not be true for an atom in which the Auger process leaves the atom in an ionized state. Our assumption implies that the electron excited in the Auger process in a metal is removed from the Fermi sea and does not significantly change the electron environment surrounding the ion deexcited by the Auger process. The failure of this assumption would add additional error to the values of E_a and E_b but not to their differences.

Error limits on values of E_F in Table I are those imposed by the resolution of our experimental data. Additional uncertainties in E_F may result from our use of a very simple model in the Auger peak analysis.

Our values of the spin-orbit splitting between $^2P_{3/2}$ and $^2P_{1/2}$ core levels agree with those observed in optical data from singly ionized Rb and Cs. They do not agree well with the values observed in optical data from neutral Rb and Cs with the atomic configurations $np^5(n+1)s^2$. This indicates that any valence electron relaxation effects that accompany the excitation of the core electrons do not substantially change the spin-orbit splittings from those observed in the free ion.

†Research supported by National Science Foundation.

[1]N. V. Smith and G. B. Fisher, Phys. Rev. B 3, 3662 (1971).

[2]N. V. Smith and W. E. Spicer, Phys. Rev. Letters 23, 769 (1969).

[3]J. F. Kenney, MIT Solid-State and Molecular Theory Group Quarterly Progress Report No. 66, 1967 (unpublished).

[4]N. V. Smith, Phys. Rev. B 2, 2840 (1970).

[5]U. S. Whang, E. T. Arakawa, and T. A. Callcott, Phys. Rev. Letters 25, 646 (1970); J. Opt. Soc. Am. 61 740 (1971).

[6]C. E. Moore, Natl. Bur. Std. (U.S.) Circular No. 467 (unpublished).

[7]T. F. Gesell and E. T. Arakawa, Phys. Rev. Letters 26, 377 (1971).

[8]R. C. Eden, Stanford University Electronics Laboratories Technical Report No. 5221-1, 1967 (unpublished).

[9]R. E. Weber, in Proceedings of the Twenty-Seventh Annual Conference on the Physics of Electronics, 1967 (unpublished).

[10]E. H. S. Burhop, *The Auger Effect and Other Radiationless Transitions* (Cambridge U. P., Cambridge, England, 1952).

[11]R. A. Rubenstein, Ph. D. thesis (University of Illinois, 1955) (unpublished).

PHYSICAL REVIEW B VOLUME 4, NUMBER 12 15 DECEMBER 1971

Photon Interactions at a Rough Metal Surface*

J. M. Elson†
Health Physics Division, Oak Ridge National Laboratory, Oak Ridge, Tennessee 37830
and
R. H. Ritchie
Health Physics Division, Oak Ridge National Laboratory, Oak Ridge, Tennessee 37830
and Department of Physics, University of Tennessee, Knoxville, Tennessee 37916
(Received 8 March 1971)

We have analyzed the processes of diffuse scattering of photons and surface-plasmon creation by photons at a rough metal surface. We have approximated the metal by an electron gas of uniform density which is bounded by a nearly plane surface at which the density falls abruptly to zero. Quantum perturbation theory is used to evaluate the probability of occurrence of the various processes at the assumed "weakly" rough surface.

I. INTRODUCTION

Collective electron polarization resonances in solids can be excited by photons and by energetic charged particles. These resonances may become manifest when photons having quantum energies in